Results in Surfaces and Interfaces 18 (2025) 100442

Contents lists available at ScienceDirect

Results in Surfaces and Interfaces

journal homepage: www.elsevier.com/locate/rsurfi

Full length article

Grand Canonical Monte Carlo simulations of the Hydrogen and Methane storage capacities of a novel Co-MOF

A. Granja-DelRío, I. Cabria *

Departamento de Física Teórica, Atómica y Óptica, Universidad de Valladolid, ES-47011, Valladolid, Spain

ARTICLE INFO

Keywords:
Hydrogen storage
Methane storage
Metal-organic frameworks
Grand Canonical Monte Carlo simulations

ABSTRACT

The creation of materials capable of efficiently storing hydrogen and methane is crucial, especially for the development of hydrogen-powered vehicles. Metal-Organic Frameworks (MOFs) have shown great promise in achieving the stringent storage targets set by the Department of Energy (DOE) for hydrogen and methane. This research uses Grand Canonical Monte Carlo (GCMC) simulations at 77 and 298.15 K and pressures between 0.5 and 25 MPa, to explore the gravimetric and volumetric hydrogen and methane storage capacities of the newly synthesized Co-MOF, named KEZBUQ. The study includes a comparative analysis of selected MOFs with similar metal compositions, as well as those with analogous density, all assessed at room temperature and moderate pressures, 25 MPa. The findings indicate that KEZBUQ exhibits significant gravimetric and volumetric storage capacities for both hydrogen and methane, outperforming many of the selected MOFs. In the case of methane, the volumetric and gravimetric storage capacities of KEZBUQ are 0.20 kg/L and 32.26 wt. %, respectively, at 298.15 K and 25 MPa, very close to the DOE targets. These results highlight the potential of KEZBUQ to enhance clean energy storage technologies. The findings suggest that this Co-MOF could offer promising performance in gas storage applications, particularly for energy storage in vehicular hydrogen tanks. Given that Co-based MOF has been relatively unexplored for gas adsorption, this study provides a foundation for further research into their potential for broader industrial applications, including energy storage and environmental gas capture.

1. Introduction

The use of fossil-based fuels implies important environmental risks. Hydrogen is crucial to move towards a carbon neutral civilization, minimizing the environmental issues (Anon, 2021; Zhang et al., 2024; Capurso et al., 2022; Abe et al., 2019; Ball and Weeda, 2015). The most common methods to store hydrogen on-board vehicles require complex infrastructure, energy and have some shortcomings. A hydrogen vehicle needs to store hydrogen in high-pressure tanks at large pressures, 70 MPa, which require heavy and expensive compressors (Hwang and Varma, 2014; Chu et al., 2023; Rasul et al., 2022; Breeze, 2018; Ding and Yakobson, 2011; Assoualaye et al., 2020). Liquid hydrogen storage requires large amounts of energy, heavy and large containers and it has evaporation losses. Methane vehicles are less pollutant than other vehicles based on fossil fuels and they could be a bridge between the present vehicles and the hydrogen fuel cell vehicle. The standarized methane tanks use pressures of 25–35 MPa (Sherburne, 2022; for Standardization, 2006). There are also standarized hydrogen tanks for pressures up to 25 MPa (Office of Energy Efficiency & Renewable Energy, Hydrogen and Fuel Cell Technologies Office, 2022).

A gas storage method that is useful to overcome the mentioned shortcomings of the gas and liquid methods is the storage of gas by physisorption on solid porous materials. This method requires lower pressures and is less expensive than other methods (Jose et al., 2023; Nath et al., 2022; Zhao et al., 2022; Forrest et al., 2022; Li, 2022; Suresh et al., 2021; Jaramillo et al., 2021; Yuan et al., 2018; Wang et al., 2018; Yuan et al., 2017; Beckner and Dailly, 2015; Yabing et al., 2014; Denysenko et al., 2014; Ci et al., 2003). Metal-Organic Frameworks (MOFs) is a group of solid porous materials that stand out as promising candidates for gas storage, primarily due to their exceptional porosity, tunable density, and large specific surface area, which collectively enhance their gas adsorption capacities.

Recently a new Co-MOF with photocatalytic properties (Zhao et al., 2023b,a) and Co-MOF/g-C_3N_4 composites, with higher photocatalytic properties, were synthesized (Zhao et al., 2023b). Two nomenclatures of this new Co-MOF are catena-[(μ-9,10-bis(4-pyridyl)anthracene)-bis (μ-2-amino[1,1'-biphenyl]-4,4'-dicarboxylato)-di-cobalt(ii) N,N-dimethylformamide solvate] and [Co(9,10-bis(4-pyridyl)anthracene)0.5(bpda)]·4DMF. The Crystallographic Database Center (CCDC) (Anon, 2024a)

* Corresponding author.
E-mail address: ivan.cabria@uva.es (I. Cabria).

https://doi.org/10.1016/j.rsurfi.2025.100442
Received 27 January 2025; Accepted 28 January 2025
Available online 5 February 2025

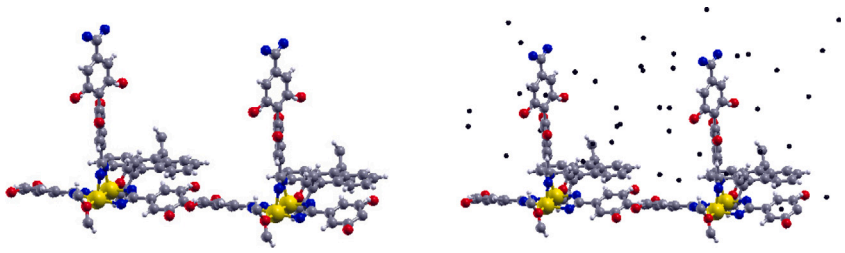

Fig. 1. The simulation cell of the KEZBUQ MOF, plotted with the xcrysden software (Kokalj, 2024). Hydrogen, carbon, nitrogen, oxygen and cobalt atoms are represented by white, gray, red, blue and yellow spheres, respectively. The hydrogen molecules are represented by black spheres.

database identifier of the new Co-based MOF is KEZBUQ (Zhao et al., 2023a). This new MOF has a low density and a high porosity and hence, it could be a promising solid porous material for another type of technological application: On-board gas storage. While KEZBUQ has been explored for its photocatalytic properties, the focus of this study is on its gas storage capabilities. Specifically, the Co-MOF KEZBUQ exhibits a highly porous structure with well-defined pore sizes and low density, which could make it particularly effective for hydrogen and methane adsorption. The structural features of KEZBUQ, rather than its photocatalytic properties, are central to its relevance as a promising material for on-board gas storage applications.

The goal of this research is to analyze and predict the hydrogen and methane usable storage capacities of KEZBUQ, a new Co-based MOF, at room temperature. Grand Canonical Monte Carlo (GCMC) simulations were utilized to calculate the usable storage capacities of KEZBUQ and two sets of MOFs. The first set includes Co-based MOFs with the same C/Co ratio as KEZBUQ, 26, while the second set consists of MOFs with similar porosity and density to KEZBUQ.

Additionally, this research investigates the correlation between the usable storage capacities and the structural properties of the simulated MOFs, such as porosity, density and pore size. This detailed understanding of the interactions between adsorbed molecules and MOFs is crucial for uncovering the origins of their storage capacities and plays a significant role in the strategic design of new MOFs.

Finally, while there has been extensive research into MOFs based on metals such as zinc, copper, and aluminium for gas storage, relatively little attention has been given to cobalt-based MOFs. This is a significant gap in the literature, as KEZBUQ might offer unique structural and chemical properties that enhance gas storage capabilities. This study addresses this gap by presenting the first detailed investigation of hydrogen and methane storage in a novel Co-based MOF. Through Grand Canonical Monte Carlo (GCMC) simulations, we provide new insights into the pressure and structural dependencies of gas adsorption in Co-MOFs, laying the groundwork for future research into their potential applications in sustainable energy storage.

2. Methodology and materials simulated

GCMC simulations were carried out to investigate the adsorption of hydrogen and methane molecules within the materials at temperatures of 77 and 298.15 K and pressures ranging from 0.5 to 25 MPa using an in-house code, named mcmgs. Most of the simulations were performed at 298.15 K. Each GCMC simulation included ten million iterations, with storage capacities calculated using the final five million iterations. The atoms within the KEZBUQ were treated as rigid entities throughout the simulations. During each iteration, three types of potential trials were considered: moving, adding, or removing a molecule. Specifically, 40 % of the trials involved removing a molecule, another 40% involved adding a molecule, and the remaining 20% involved moving a molecule. These trial percentages were established through multiple preliminary test simulations.

The interactions between molecules and atoms have been calculated by means of the Lennard–Jones (LJ) interaction potential energy (Lennard-Jones, 1924). The LJ parameters ϵ and σ used in the simulations are in Table S1 in the Supplementary Information. Most of the results of the present research have been obtained using the set of LJ parameters in Table S1. However, to compare the results with well-known force-fields, a few GCMC simulations have been also performed with a second set of LJ coefficients that uses for methane the LJ TraPPE coefficients (Anon, 2024c) and for H_2 the LJ coefficients published by Darkrim and Levesque (1998) (See Table S2 in the Supplementary Information).

The Feynman–Hibbs correction (Feynman and Hibbs, 1965) was employed to include the quantum effects into the interaction potential and it was applied to all GCMC simulations reported in this paper: at 77 K and also at room temperature. The Soave–Redlich–Kwong (SRK) equation of state of hydrogen and methane was used to calculate the chemical potential (Soave, 1972). This is a cubic equation that provides accurate values of the properties of hydrogen, methane and other gases (Bertucco and Fermeglia, 2023). Two gas usable storage capacities, volumetric and gravimetric, and the isosteric heat of adsorption, Q_{st}, are calculated in the GCMC simulations, according to the definitions previously published (Cabria, 2024). The porosity and pore radii of the pores of the MOFs have been calculated using an algorithm or procedure previously published and explained (Cabria, 2024; Granja-DelRío and Cabria, 2024b). These structural parameters depend on the type of gas. They have, in general, different values for hydrogen and methane. The specific surface area, SSA, and specific pore volume of the MOFs have been calculated using the Zeo++ open software (Haranczyk, 2024; Ongari et al., 2017; Martin and Haranczyk, 2014; Pinheiro et al., 2013b,a; Martin et al., 2012; Willems et al., 2012).

Two groups of MOFs were selected from the CCDC database. A group of MOFs with the same C/Co ratio as KEZBUQ and density equal or below 0.8 kg/L was selected from the CCDC MOF subset. This group is named 'C/Co=26' throughout this paper. That group is composed by the MOFs with the following CCDC identifiers: LAFQOA, LAFQUG, LAFRER, LAFRIV, LAFROB, LAXJAX, PUZLOM, PUZLUS, PUZMAZ, RIFSOQ, RIVDEH and ZAGFOF. A group of MOFs with density and porosity similar to those of KEZBUQ is composed by the MOFs with the following CCDC identifiers: SECSUR, VAGMAT, XAFFAN, XAFFIV and XAFFOB.

The simulation cells of the all the MOFs were obtained from their Crystallographic Information File (CIF) format files in the CCDC database (Anon, 2024a). The simulation cells of the two selected sets of MOFs were obtained from the MOF CCDC subset (Li et al., 2021). The simulation cell of KEZBUQ was obtained from the general CCDC database. Fig. 1 is a depiction of the simulation cell of KEZBUQ. The right panel of that figure includes the locations of hydrogen molecules obtained in GCMC simulations at 298.15 K and 25 MPa. The GCMC simulations were carried out for all MOFs under the same temperature, pressures and conditions, as detailed earlier. This process facilitates a meaningful evaluation and comparison of their respective usable storage capacities.

To assess the intensity and type of the adsorption of a molecule on the KEZBUQ structure, Density Functional Theory, DFT, calculations of the interaction of a single hydrogen molecule with KEZBUQ have been carried out using the Quantum Espresso, QE, code, version

Table 1
Total hydrogen and methane storage capacities of some MOFs at different temperatures and pressures. Results include RASPA simulations and experimental values from other groups. Pressure P is in MPa, temperature T in K, gravimetric capacity g_c in wt. % and v_c in kg/L.

MOF	Gas	P	T	Technique	g_c	v_c	Source
IRMOF-1	H_2	10	298	RASPA	1.35	0.0094	Assoualaye et al. (2020)
IRMOF-1	H_2	10	298	mcmgs	1.14	0.0069	
IRMOF-1	CH_4	3.6	300	exps.	13.5	0.0787	Zhou et al. (2007)
IRMOF-1	CH_4	3.6	300	mcmgs	12.3	0.0837	
IRMOF-1	CH_4	4.5	298	RASPA	12.3		Rodrigues et al. (2022)
IRMOF-1	CH_4	4.5	298	mcmgs	14.7		
MOF-177	CH_4	10	298	exps.	22.0		Saha and Deng (2010)
MOF-177	CH_4	10	298	mcmgs	26.6		
HKUST-1	CH_4	6.5	298	exps.	17.8	0.1910	Peng et al. (2013)
HKUST-1	CH_4	6.5	298	mcmgs	15.4	0.1724	
NU-125	CH_4	6.5	298	exps.	22.3	0.1659	Peng et al. (2013)
NU-125	CH_4	6.5	298	mcmgs	20.5	0.1570	
Al-nia-MOF-1	CH_4	8	258	exps.	28.6	0.1880	Alezi et al. (2022)
Al-nia-MOF-1	CH_4	8	258	mcmgs	29.1	0.2010	Granja-DelRío and Cabria (2024a)
Al-nia-MOF-1	CH_4	8	273	exps.	24.5	0.1660	Alezi et al. (2022)
Al-nia-MOF-1	CH_4	8	273	mcmgs	27.6	0.1870	Granja-DelRío and Cabria (2024a)
Al-nia-MOF-1	CH_4	8	298	exps.	23.1	0.1420	Alezi et al. (2022)
Al-nia-MOF-1	CH_4	8	298	mcmgs	24.8	0.1610	Granja-DelRío and Cabria (2024a)

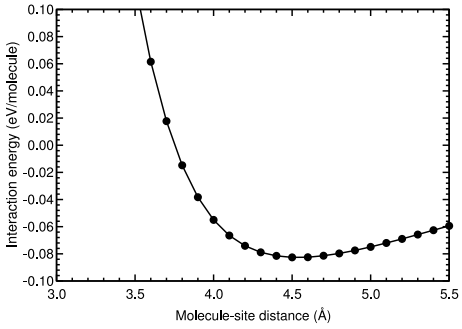

Fig. 2. Interaction energy of a single hydrogen molecule with KEZBUQ, as a function of the radial distance between the molecule and one of the metal sites of KEZBUQ, two bonded Co atoms.

6.7 (Giannozzi et al., 2017, 2009; Anon, 2024b). The PBE-D3 functional (Grimme et al., 2010) has been used, because that functional includes the dispersion interactions, which are relevant to study the adsorption of molecules on surfaces. The kinetic energy cutoff for wavefunctions used in these calculations was 84 Ry. The kinetic energy cutoff for charge density and potential was four times the cutoff for wavefunctions. The convergence threshold on total energy and for self consistency were both equal to 10^{-6} Ry. These values of the parameters of the QE calculations were chosen after running several tests.

An analysis of the charges on the atoms and the hydrogen molecule was also performed, using the QE code. The Löwdin charge analysis was chosen (Löwdin, 1950). The KEZBUQ MOF contains H, C, N, O and Co atoms. According to the Löwdin charge analysis, the net charges on H, C, N, O and Co atoms were, on average and e units: 0.058, −0.117, −0.017, −0.105 and 4.479, respectively. The net charge on each H atom of the hydrogen molecule itself was −0.08 e.

The interaction energy $E(d)$ between KEZBUQ and a hydrogen molecule located at a radial distance d from the center of one of the metal sites of KEZBUQ, which consists of two bonded Co atoms (two big yellow neighbor spheres in Fig. 1), is defined as:

$$E(d) = E(\mathrm{H_2\ on\ KEZBUQ};d) - E(\mathrm{H_2}) - E(\mathrm{KEZBUQ})\,, \quad (1)$$

In Fig. 2 we have plotted the interaction energy as a function of the mentioned radial distance. The binding energy is about 0.083 eV/molecule, which indicates that the interactions are weak and is a binding energy similar to the binding energies of the LJ potentials used in the simulations.

3. Comparison of hydrogen and methane storage capacities with other simulation and experimental results

Tables 1–3 contain total and usable hydrogen and methane storage capacities of several MOFs obtained from simulations and experiments from another research groups at temperatures between 270 and 300 K. They are compared with the capacities obtained using the mcmgs code, the code used in the present work to carry out the GCMC simulations.

The total hydrogen gravimetric and volumetric capacities calculated by the RASPA and mcmgs codes show small differences. The mcmgs capacities are only about 20% and 36% smaller than the values obtained from the RASPA code for gravimetric and volumetric capacities, respectively. In the methane case, RASPA and mcmgs capacities are quite similar as well as experimental capacities. Below 10 MPa, the experimental gravimetric capacities are only slightly higher than the mcmgs capacities, about 10%–15% higher. Similar differences can be found between the RASPA and mcmgs total gravimetric capacities. The differences between the experimental and mcmgs total volumetric capacities are relatively small, about 10%. As regards the usable methane capacities at temperatures between 270 and 298, the differences between the experimental and mcmgs usable capacities are small and are in the range 5%–20%.

4. Usable hydrogen and methane storage capacities as a function of structural parameters

The hydrogen usable storage capacities of KEZBUQ and the two groups of MOFs vs the porosity, density, largest pore radius and average pore radius are plotted in Figs. 3–6. Those are the storage capacities obtained in the GCMC simulations at 298.15 K and 25 MPa.

The usable hydrogen volumetric capacities in Fig. 3 range from 0.012 to 0.016 kg/L and the gravimetric capacities are within the interval 1.6–4.0 wt. %. As regards usable methane capacities, the volumetric capacities are within the interval 0.09–0.21 kg/L and the gravimetric capacities within the interval 10–35 wt. %. The densities of the solid porous materials studied are between 0.3 and 0.8 kg/L. The porosities of the materials studied in Fig. 4 fall within the interval 0.2–0.6.

The usable (hydrogen or methane) storage capacities of the studied MOFs decrease as the density increases. The dependence of the capacities on the density is approximately linear (See Fig. 3). In the case of hydrogen that dependence is practically linear. This is a general trend found in all the solid porous materials. The usable gas (hydrogen or methane) storage capacities of the MOFs increase with the porosity. The dependence of the capacities on the porosity is practically linear

Table 2
Usable methane storage capacities of NU-1501-Al and NU-1501-Fe MOFs at different temperatures and pressures obtained in experiments from other groups and in the present GCMC simulations. Pressure P is in MPa, temperature T in K, gravimetric capacity g_c in wt. % and v_c in kg/L.

MOF	Gas	P	T	Technique	g_c	v_c	Source
NU-1501-Al	CH_4	8	273	exps.	35.1	0.1545	Chen et al. (2020)
NU-1501-Al	CH_4	8	273	mcmgs	36.2	0.1921	
NU-1501-Al	CH_4	10	273	exps.	37.5	0.1702	Chen et al. (2020)
NU-1501-Al	CH_4	10	273	mcmgs	37.8	0.2061	
NU-1501-Al	CH_4	8	298	exps.	31.0	0.1252	Chen et al. (2020)
NU-1501-Al	CH_4	8	298	mcmgs	31.8	0.1584	
NU-1501-Al	CH_4	10	298	exps.	33.3	0.1395	Chen et al. (2020)
NU-1501-Al	CH_4	10	298	mcmgs	34.4	0.1779	
NU-1501-Fe	CH_4	8	273	exps.	33.8	0.1545	Chen et al. (2020)
NU-1501-Fe	CH_4	8	273	mcmgs	32.0	0.1671	
NU-1501-Fe	CH_4	10	273	exps.	36.5	0.1717	Chen et al. (2020)
NU-1501-Fe	CH_4	10	273	mcmgs	34.0	0.1827	
NU-1501-Fe	CH_4	8	298	exps.	29.6	0.1252	Chen et al. (2020)
NU-1501-Fe	CH_4	8	298	mcmgs	28.3	0.1404	
NU-1501-Fe	CH_4	10	298	exps.	32.4	0.1431	Chen et al. (2020)
NU-1501-Fe	CH_4	10	298	mcmgs	30.9	0.1585	

Table 3
Usable methane storage capacities of Al-soc-MOF-1, NU-111 and PCN-14 MOFs at different temperatures and pressures obtained in experiments from other groups and in the present GCMC simulations. Pressure P is in MPa, temperature T in K, gravimetric capacity g_c in wt. % and v_c in kg/L.

MOF	Gas	P	T	Technique	g_c	v_c	Source
Al-soc-MOF-1	CH_4	6.5	270	exps.	31.0	0.1516	Alezi et al. (2015)
Al-soc-MOF-1	CH_4	6.5	270	mcmgs	28.2	0.1455	
Al-soc-MOF-1	CH_4	8	273	exps.	33.3	0.1702	Chen et al. (2020)
Al-soc-MOF-1	CH_4	8	273	mcmgs	30.0	0.1588	
Al-soc-MOF-1	CH_4	6.5	298	exps.	27.0	0.1109	Alezi et al. (2015)
Al-soc-MOF-1	CH_4	6.5	298	mcmgs	24.1	0.1175	
Al-soc-MOF-1	CH_4	8	298	exps.	29.6	0.1431	Alezi et al. (2015)
Al-soc-MOF-1	CH_4	8	298	mcmgs	26.3	0.1323	
NU-111	CH_4	6.5	270	exps.	23.7	0.1259	Alezi et al. (2015)
NU-111	CH_4	6.5	270	mcmgs	22.3	0.1236	
NU-111	CH_4	6.5	298	exps.	23.5	0.1252	Alezi et al. (2015)
NU-111	CH_4	6.5	298	mcmgs	18.5	0.0976	
PCN-14	CH_4	6.5	270	exps.	10.7	0.1001	Alezi et al. (2015)
PCN-14	CH_4	6.5	270	mcmgs	8.7	0.0833	
PCN-14	CH_4	6.5	298	exps.	11.5	0.1116	Alezi et al. (2015)
PCN-14	CH_4	6.5	298	mcmgs	9.6	0.0919	

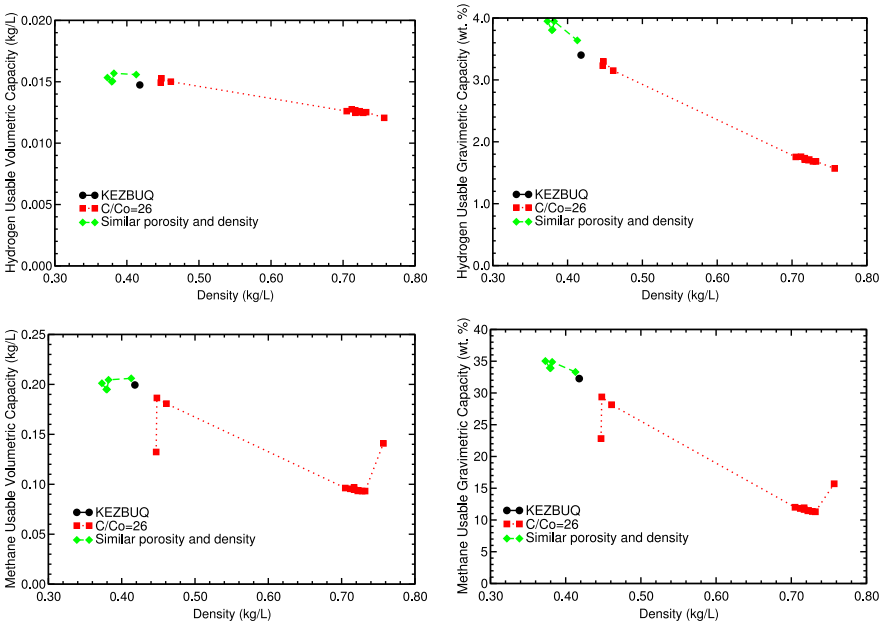

Fig. 3. Usable hydrogen and methane volumetric and gravimetric capacities at 298.15 K and 25 MPa vs density.

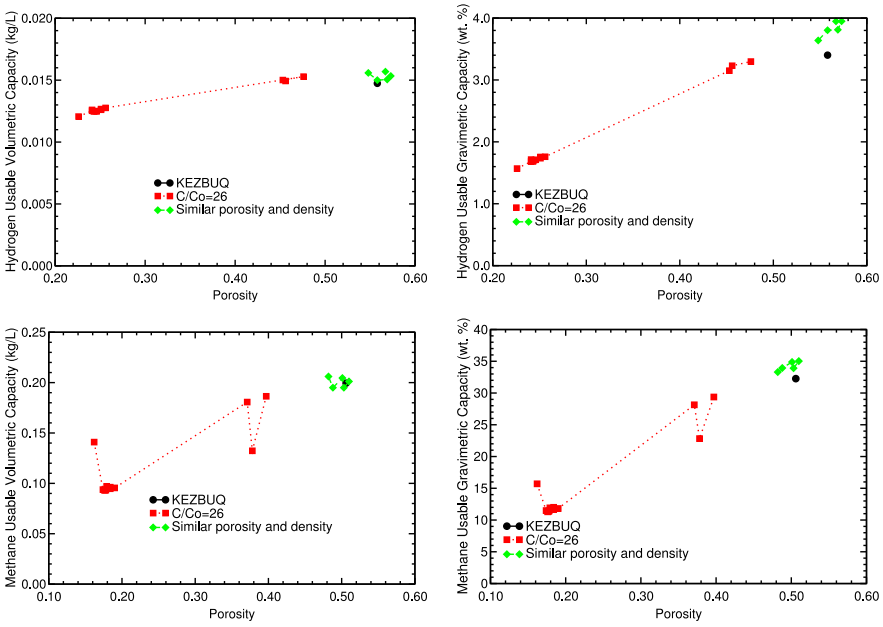

Fig. 4. Usable hydrogen and methane volumetric and gravimetric capacities at 298.15 K and 25 MPa vs porosity.

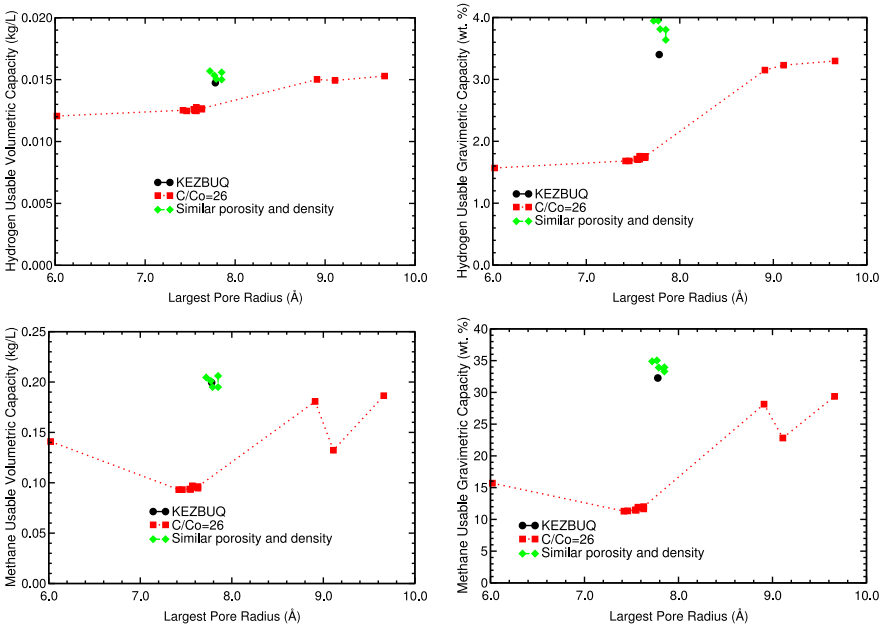

Fig. 5. Usable hydrogen and methane volumetric and gravimetric capacity at 298.15 K and 25 MPa vs largest pore radius.

in the case of hydrogen and approximately linear in the case of methane (See Fig. 4).

As can be noticed in Figs. 3 and 4, the MOFs with the same C/Co ratio, i.e., KEZBUQ and the 'C/Co=26' group, do not have similar hydrogen or methane storage capacities. In fact, their usable storage capacities depend on their density and not on the C/Co ratio. The MOFs with similar density or porosity than KEZBUQ have also similar storage capacities, although they do not have Co and/or have a different C/Co ratio. These results indicate that density and porosity of the solid porous materials are more significant than the C/Co ratio, for hydrogen storage capacities.

The dependence of the storage capacities on the largest pore radius is plotted in Fig. 5 and the dependence on the average pore radius is plotted in Fig. 6. The largest pore radius of the MOFs studied is between 6 and 10 Å and the average pore radius is between 3 and 9 Å. The storage capacities increase, in general, as the largest pore radius of the MOF increases. That trend is more clear in the case of hydrogen capacities and less clear in the case of methane capacities. The dependence of the storage capacities on the average pore radius of the studied MOFs seems to be parabolic, with the apex of the parabolic function around 4-5 Å (See Fig. 6).

In Fig. 5 it can be found that the MOFs with density and porosity similar to those of KEZBUQ have also very similar values of the largest pore radius. Their average pore radii, however, are less similar: They are within an interval of about 2 Å (See Fig. 6). It can be also noticed in Fig. 5 that the MOFs with a similar largest pore radius, do not have necessarily similar storage capacities. Only the MOFs with similar density, porosity and largest pore radius have also similar storage capacities.

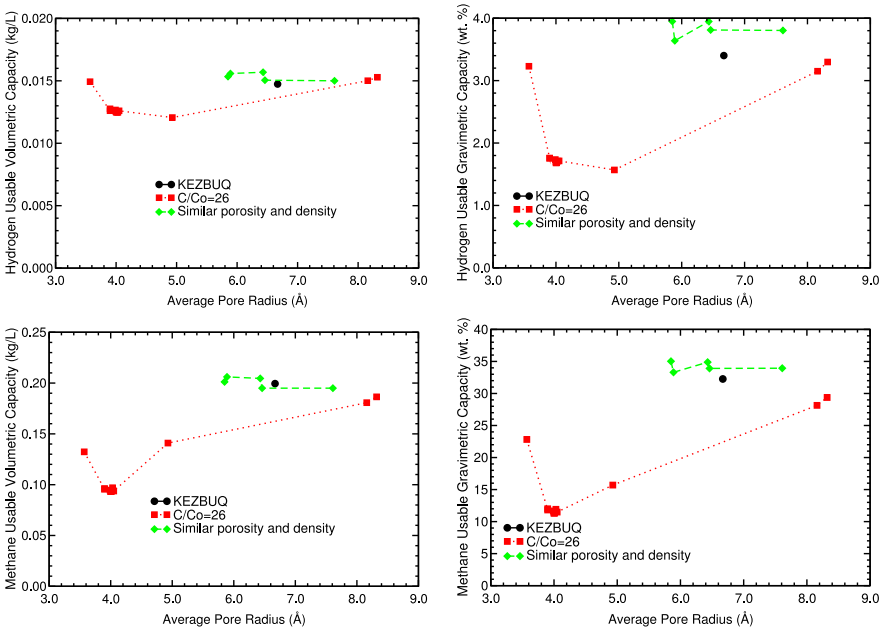

Fig. 6. Usable hydrogen and methane volumetric and gravimetric capacity at 298.15 K and 25 MPa vs average pore radius.

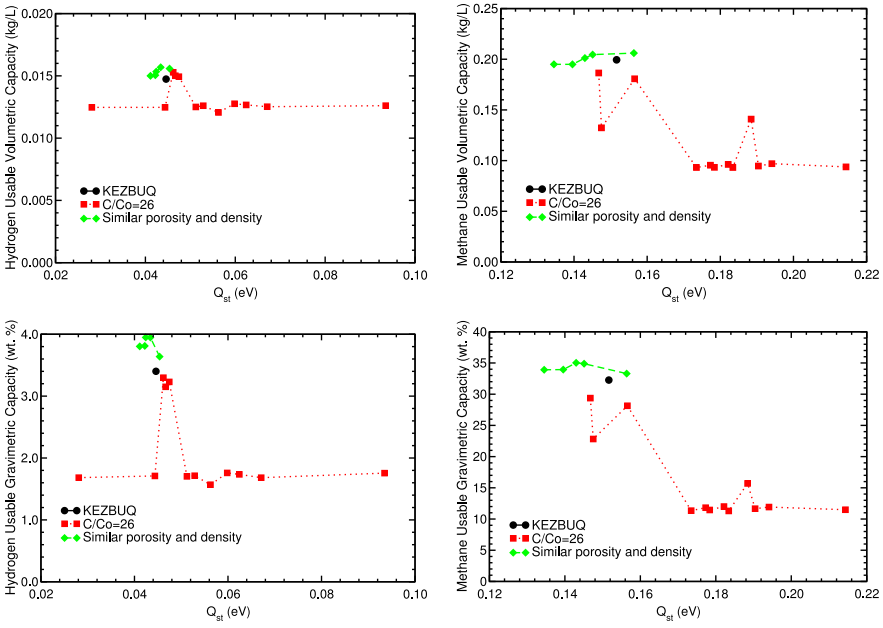

Fig. 7. Usable hydrogen and methane volumetric and gravimetric capacity at 298.15 K and 25 MPa vs isosteric heat.

As regards the group of MOFs with C/Co=26, Figs. 5 and 6 show that a subgroup of eight MOFs with C/Co=26 have very similar storage capacities, largest pore radius and average pore radius. The other four MOFs with C/Co=26 have different or very different values of the storage capacities, largest pore radius and average pore radius. Finally, it can be concluded from those two figures that the storage capacities of the MOFs depend strongly on the pore radii and that the C/metal ratio is not determinant.

The isosteric heat of adsorption, which reflects the strength of the interaction between the gas molecules and the adsorbent material and the local details of the structure of the adsorbent material, is related to the storage capacities, the porosity and the density of the material. Therefore, it seems logical to analyze the relationship between the isosteric heat of adsorption and those properties of these materials. In Fig. 7, the storage capacities are plotted vs the isosteric heat of hydrogen and methane.

The isosteric heats of hydrogen adsorption for the porous materials studied at 298.15 K and 25 MPa, as derived from the present GCMC simulations, range between 0.02 and 0.10 eV, while the isosteric heats of methane adsorption are within the interval 0.13–0.22 eV. It can be noticed in that figure that the dependence of the storage capacities on the isosteric heat is not clear. For some groups of MOFs the capacities do not depend on the isosteric heat: The capacities remain almost constant as the isosteric heat changes. Another groups have a strong dependence on the isosteric heat.

The isosteric heats of hydrogen adsorption of KEZBUQ and selected MOFs as a function of the porosity and the density, obtained from GCMC simulations, are plotted in Fig. 8. The isosteric heat generally rises with increasing density, though not in a strictly linear fashion. It fluctuates, showing an overall upward trend. Conversely, as porosity

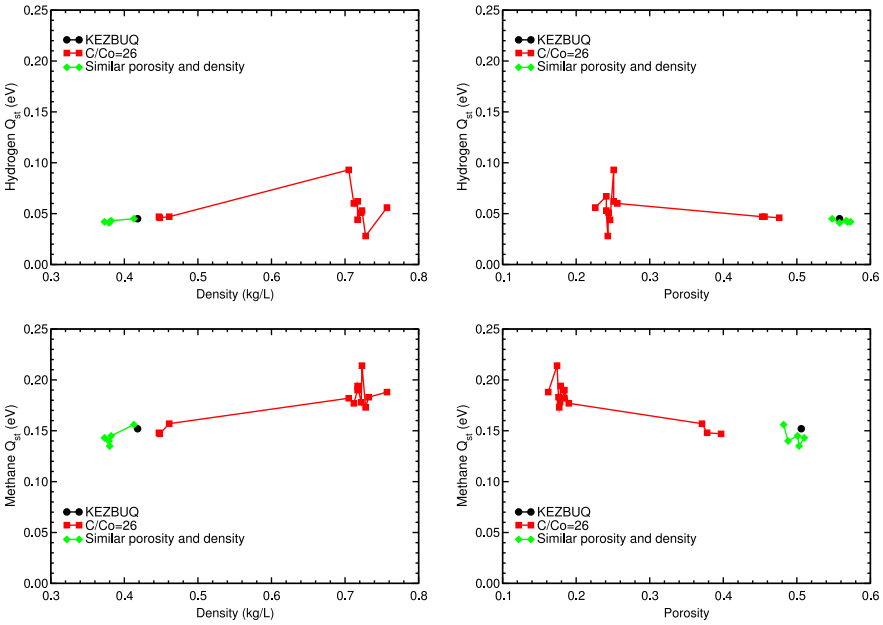

Fig. 8. Isosteric heat of adsorption, Q_{st}, of hydrogen and methane at 298.15 K and 25 MPa vs density and porosity.

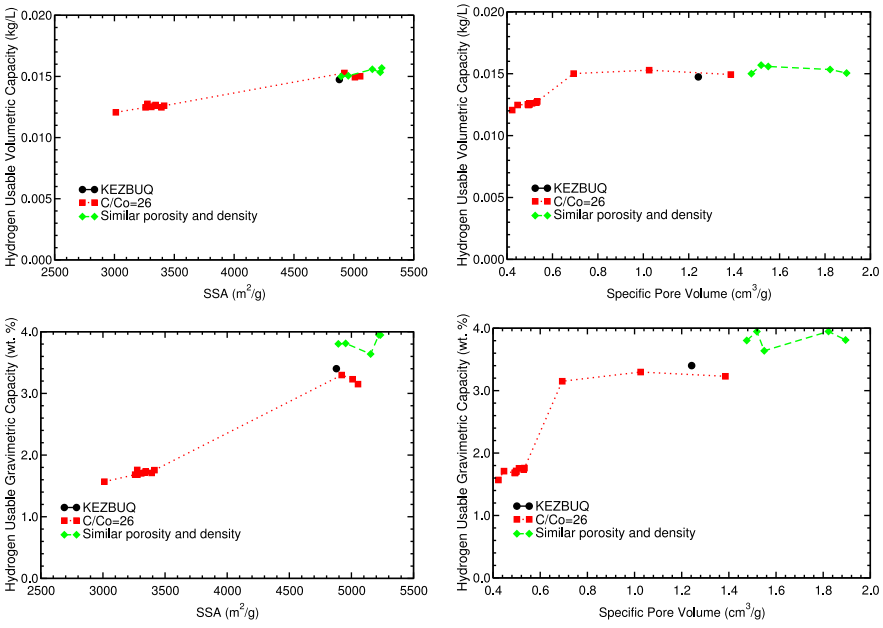

Fig. 9. Usable hydrogen volumetric and gravimetric capacity at 298.15 K and 25 MPa vs the specific surface area and the specific pore volume.

increases, the isosteric heat tends to decrease. However, the relationship with this variable is not uniform, exhibiting numerous oscillations around a decreasing average trend.

The dependence of the usable hydrogen storage capacities on the specific surface area, SSA, and on the specific pore volume is plotted in Fig. 9. The SSAs of the MOFs studied are between 3000 and 5500 m^2/g and the specific pore volumes are in the interval 0.4–2.0 cm^3/g.

The hydrogen capacities of all the MOFs studied depends linearly on the specific surface area (See Fig. 9). The hydrogen capacities increase rapidly with the specific pore volume and then, they tend towards a constant value. These trends are more clearly defined in the case of the volumetric capacities. The SSA of the KEZBUQ MOF is high, which is consistent with the high values of the storage capacities of the KEZBUQ MOF.

5. Usable hydrogen and methane storage capacities as a function of pressure

The Department of Energy, DOE, set on-board volumetric and gravimetric hydrogen storage targets for 2025 at 0.040 kg/L and 5.5 wt %, respectively (Office of Energy Efficiency & Renewable Energy, Fuel Cell Technologies Office, 2018). The ultimate storage goals are even higher, aiming for 0.050 kg H_2/L and 6.5 wt. %. There are also storage goals for on-board methane storage. The Department of Energy's Advanced Research Projects Agency - Energy (ARPA-E) established specific targets for on-board methane storage: A volumetric capacity of 0.25 kg of methane per liter and a gravimetric capacity of 33.3 wt. % at room temperature and moderate pressures (Beckner and Dailly, 2015; Yabing et al., 2014; Advanced Research Projects Agency Energy, 2012; Advanced Research Projects Agency - Energy, Department of Energy,

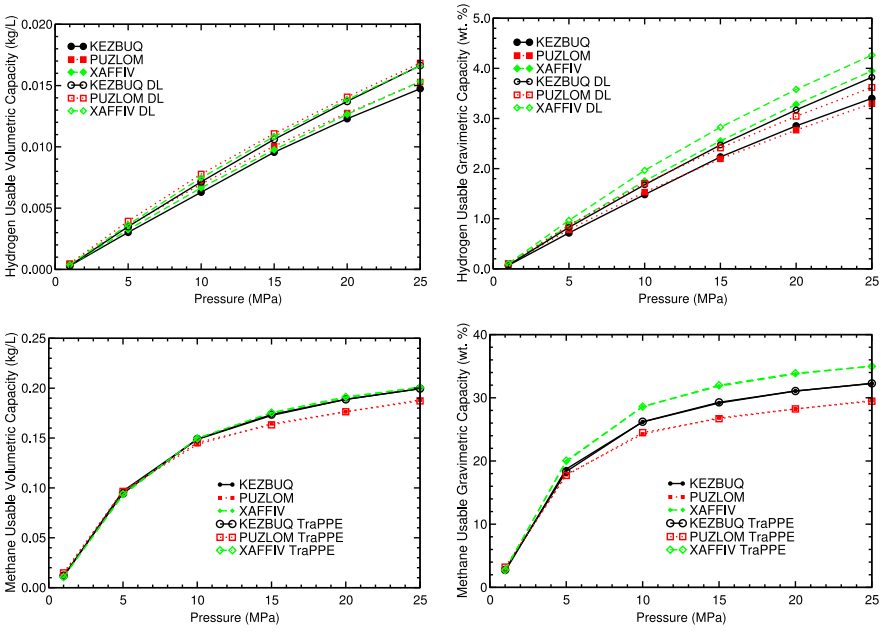

Fig. 10. Usable hydrogen (above) and methane (below) volumetric and gravimetric capacities vs pressure at room temperature using the two sets of LJ coefficients.

2012; for Standardization, 2006).

The hydrogen and methane usable storage capacities of KEZBUQ have been compared in Fig. 10 with the storage capacities of the best MOFs of the two groups of MOFs, PUZLOM and XAFFIV, which have the highest capacities of their respective groups. The hydrogen gravimetric and volumetric capacities in Fig. 10 are in the ranges 0–0.015 kg/L and 0–4 wt. %, respectively, and the methane gravimetric and volumetric capacities are in the ranges 0–0.20 kg/L and 0–35 wt. %, respectively.

The usable hydrogen and methane storage capacities of the KEZBUQ, PUZLOM and XAFFIV obtained in the GCMC simulations with the first and the second LJ sets (See Tables S1 and S2, respectively) are also compared in Fig. 10. The hydrogen capacities obtained with the second LJ set are between 0 and 12% higher than the capacities obtained with the first set. However, the methane capacities obtained with the two sets of LJ coefficients are very similar.

The hydrogen usable volumetric capacities of the three materials are very similar for any value of the pressure. The volumetric capacity of KEZBUQ would reach the DOE target for 2025, 0.040 kg/L (Office of Energy Efficiency & Renewable Energy, Fuel Cell Technologies Office, 2018), at 60–70 MPa. The gravimetric capacities of the three materials are relatively similar. The gravimetric capacity of KEZBUQ would reach the DOE target, 5.5 wt. %, at approximately 40 MPa. The hydrogen usable storage capacities of KEZBUQ are high at moderate pressures, but below the DOE targets. Probably, a new material based on KEZBUQ, but with the appropriate metal doping, could reach the DOE targets for hydrogen at lower pressures.

In the case of methane storage, the usable methane storage capacities of the three materials are also similar. The usable volumetric capacity of KEZBUQ is 0.20 kg/L at 298.15 K and 25 MPa, close to the ARPA-E target, 0.25 kg/L. It is approximately 80% of that target. The gravimetric usable capacity of KEZBUQ is 32.3 wt. % at 298.15 K and 25 MPa, almost reaching the ARPA-E target, 33.3 wt. %. Hence, this new Co-based MOF is a good candidate for on-board methane storage.

Finally, GCMC simulations of the total hydrogen volumetric and gravimetric storage capacities at 77 K are presented in Fig. 11. The volumetric and gravimetric capacities fall within the intervals 0–0.060 kg/L and 0–13 wt. %, respectively. The total volumetric capacity of KEZBUQ reaches 0.040 kg/L at 5 MPa, continuing to increase to approximately 0.060 kg/L at 25 MPa. The gravimetric capacity reaches 5.5 wt. % at around 3 MPa, and continues rising until it plateaus at 12 wt. % at 20 MPa. KEZBUQ's hydrogen storage capacities are significant at low pressures and temperatures, achieving the DOE targets.

6. Conclusions

GCMC simulations of the hydrogen and methane storage capacities of a new Co-based MOF, called KEZBUQ in the CCDC database, and of the two groups of MOFs with some structural or composition similarity with KEZBUQ have been carried out at room temperature and pressures between 0.5 and 25 MPa. According to the present analysis of the results of the GCMC simulations, the density, the porosity and the pore radii of the MOFs are much more relevant than the cobalt content or the C/Co ratio for the storage capacities.

According to the GCMC simulations, KEZBUQ has high usable storage capacities due to its low density and high porosity. In the case of methane, KEZBUQ has usable methane volumetric and gravimetric storage capacities of 0.20 kg/L and 32.3 wt. %, respectively, at 298.15 K and 25 MPa, close to or almost reaching the ARPA-E respective methane storage targets: 0.25 kg/L and 33.3 wt. %. Hence, this new Co-based MOF could be an important solid porous material for on-board methane storage.

This research offers several novel contributions to the field of gas storage in MOFs. First, it represents the pioneering study of hydrogen and methane storage capacities in newly developed Co-based MOFs, using GCMC simulations. The findings reveal a distinctive pressure-dependent behavior in storage capacity, providing important insights for optimizing operational conditions. Additionally, the role of structural properties, such as density, porosity, and pore size, was analyzed in detail, showing how these factors critically affect gas adsorption.

Perhaps most notably, Co-based MOFs demonstrated higher storage capacities under specific conditions compared to other MOFs commonly reported in the literature, positioning them as strong candidates for future energy storage solutions. The potential for optimizing these materials further through structural adjustments or bimetallic configurations opens new avenues for research and practical application.

In this study, the hydrogen and methane storage capacities were simulated using the GCMC methodology. While these simulations provide a powerful tool for predicting gas adsorption behavior and have been compared with experiments, several limitations must be acknowledged. First, the simulations rely on simplified models of the physical interactions, which may differ from the behavior of gases on some MOFs. Additionally, the pressure and temperature ranges explored in this study may not fully capture the performance across all possible

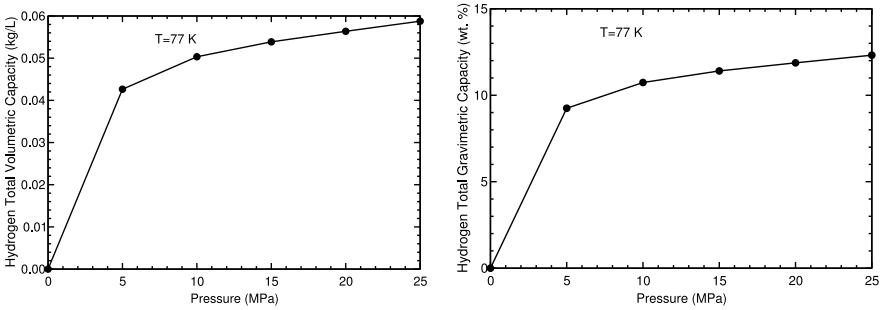

Fig. 11. Total hydrogen volumetric and gravimetric capacities vs pressure at 77 K of KEZBUQ MOF.

pressure and temperature conditions. The impact of defects, impurities, kinetic effects, and non-equilibrium behavior were also neglected in the model. Therefore, future work should include more experimental validations, investigate the impact of defects and/or impurities and explore a broader range of pressure and temperature conditions to further substantiate these findings.

CRediT authorship contribution statement

A. Granja-DelRío: Conceptualization, Data curation, Formal analysis, Investigation, Methodology, Resources, Software, Supervision, Validation, Visualization, Writing – original draft, Writing – review & editing. **I. Cabria:** Conceptualization, Data curation, Formal analysis, Investigation, Methodology, Resources, Software, Supervision, Validation, Visualization, Writing – original draft, Writing – review & editing.

Declaration of competing interest

The authors declare that they have no known competing financial interests or personal relationships that could have appeared to influence the work reported in this paper.

Acknowledgments

This work has been funded by the MICINN research project from Spain (Grant PGC2018-093745-B-I00), the Junta de Castilla y León (Grant VA124G18), and the University of Valladolid, Spain. The authors gratefully acknowledge the financial support provided by these institutions, which made this research possible. The authors would also like to express their appreciation for the use of the computer facilities at the Centro de Procesado de Datos - Parque Científico of the University of Valladolid. The xcrysden (Kokalj, 2024) and grace (Turner and Grace Development Team, 2024) software have been used to plot the simulation cell of the solid porous material and the graphs, respectively.

Appendix A. Supplementary data

Supplementary material related to this article can be found online at https://doi.org/10.1016/j.rsurfi.2025.100442.

Data availability

Data will be made available on request.

References

Abe, J.O., Popoola, A.P.I., Ajenifuja, E., Popoola, O.M., 2019. Hydrogen energy, economy and storage: Review and recommendation. Int. J. Hydrog. Energy 44, 15072–15086. http://dx.doi.org/10.1016/j.ijhydene.2019.04.068.

Advanced Research Projects Agency - Energy, Department of Energy, 2012. Methane opportunities for vehicular energy (MOVE). https://arpa-e.energy.gov/technologies/programs/move, (Accessed 28 December 2024).

Advanced Research Projects Agency Energy, D.o.E., 2012. Methane opportunities for vehicular energy (MOVE) program overview. http://arpa-e.energy.gov/sites/default/files/documents/files/MOVE_ProgramOverview.pdf, (Accessed 28 December 2024).

Alezi, D., Belmabkhout, Y., Suyetin, M., Bhatt, P.M., Weseliński, L.J., Solovyeva, V., Adil, K., Spanopoulos, I., Trikalitis, P.N., Emwas, A.-H., Eddaoudi, M., 2015. MOF crystal chemistry paving the way to gas storage needs: Aluminum-based soc-MOF for CH_4, o_2, and CO_2 storage. J. Am. Chem. Soc. 137, 13308–13318. http://dx.doi.org/10.1021/jacs.5b07053.

Alezi, D., Jia, J., Bhatt, P.M., Shkurenko, A., Solovyeva, V., Chen, Z., Belmabkhout, Y., Eddaoudi, M., 2022. Reticular chemistry for the construction of highly porous aluminum-based nia-metal-organic frameworks. Inorg. Chem. 61 (28), 10661–10666. http://dx.doi.org/10.1021/acs.inorgchem.2c00756.

Anon, 2021. Net zero by 2050. a roadmap for the global energy sector. https://www.iea.org/reports/net-zero-by-2050, (Accessed 28 December 2024).

Anon, 2024a. Cambridge crystallographic database centre. (Accessed 28 December 2024).

Anon, 2024b. Quantum Espresso: an integrated suite of open-source computer codes for electronic-structure calculations and materials modeling at the nanoscale. It is based on density-functional theory, plane waves, and pseudopotentials. (Accessed 28 December 2024), Last version: 7.3, January 9, 2024.

Anon, 2024c. Transferable Potentials for Phase Equilibria. TraPPE-United Atom. (Accessed 28 December 2024).

Assoualaye, G., Tom, A., Djongyang, N., 2020. Monte Carlo study of hydrogen adsorption by MOF-5 doped with cobalt at ambient temperature and pressure. SN Appl. Sci. 2, 1815. http://dx.doi.org/10.1007/s42452-020-03627-9.

Ball, M., Weeda, M., 2015. The hydrogen economy-vision or reality? Int. J. Hydrog. Energy 40, 7903–7919.

Beckner, M., Dailly, A., 2015. Adsorbed methane storage for vehicular applications. Appl. Energy 149, 69–74. http://dx.doi.org/10.1016/j.apenergy.2015.03.123.

Bertucco, A., Fermeglia, M., 2023. 50 years of Soave equation of state (SRK): A source of inspiration for chemical engineers. Fluid Phase Equilib. 566, 113678. http://dx.doi.org/10.1016/j.fluid.2022.113678.

Breeze, P., 2018. Hydrogen energy storage. In: Power System Energy Storage Technologies. Elsevier, London, pp. 69–77.

Cabria, I., 2024. Grand canonical Monte Carlo simulations of the hydrogen and methane storage capacities of novel BUT MOFs at room temperature. Int. J. Hydrog. Energy 50, 160–177. http://dx.doi.org/10.1016/j.ijhydene.2023.06.298.

Capurso, T., Stefanizzi, M., Torres, M., Camporeale, S.M., 2022. Review perspective of the role of hydrogen in the 21st century energy transition. Energy Convers. Manag. 251, 114898.

Chen, Z., Li, P., Anderson, R., Wang, X., Zhang, X., Robison, L., Redfern, L.R., Moribe, S., Islamoglu, T., Gómez-Gualdrón, D.A., Yildirim, T., Stoddart, J.F., Farha, O.K., 2020. Balancing volumetric and gravimetric uptake in highly porous materials for clean energy. Science 368, 297–303. http://dx.doi.org/10.1126/science.aaz8881.

Chu, C., Wu, K., Luo, B., Cao, Q., Zhang, H., 2023. Hydrogen storage by liquid organic hydrogen carriers: Catalyst, renewable carrier, and technology – a review. Carbon Resour. Convers. 6 (4), 334–351. http://dx.doi.org/10.1016/j.crcon.2023.03.007.

Ci, L., Zhu, H., Wei, B., Xu, C., Wu, D., 2003. Annealing amorphous carbon nanotubes for their application in hydrogen storage. Appl. Surf. Sci. (ISSN: 0169-4332) 205 (1), 39–43. http://dx.doi.org/10.1016/S0169-4332(02)00897-8.

Darkrim, F., Levesque, D., 1998. Monte Carlo simulations of hydrogen adsorption in single-walled carbon nanotubes. J. Chem. Phys. 109, 4981–4984.

Denysenko, D., Grzywa, M., Jelic, J., Reuter, K., Volkmer, D., 2014. Scorpionate-type coordination in MFU-4l metal–organic frameworks: Small-molecule binding and activation upon the thermally activated formation of open metal sites. Angew. Chem. Int. Ed. 53 (23), 5832–5836. http://dx.doi.org/10.1002/anie.201310004.

Ding, F., Yakobson, B.I., 2011. Challenges in hydrogen adsorptions: from physisorption to chemisorption. Front. Phys. 6, 142–150. http://dx.doi.org/10.1007/s11467-011-0171-6.

Feynman, R.P., Hibbs, A., 1965. Quantum Mechanics and Path Integrals. McGraw-Hill, New York.

Forrest, K.A., Verma, G., Ye, Y., Ren, J., Ma, S., Pham, T., Space, B., 2022. Methane storage in flexible and dynamical metal–organic frameworks. Chem. Phys. Rev. 3 (2), 021308. http://dx.doi.org/10.1063/5.0072805.

Giannozzi, P., Andreussi, O., Brumme, T., Bunau, O., Nardelli, M.B., Calandra, M., Car, R., Cavazzoni, C., Ceresoli, D., Cococcioni, M., Colonna, N., Carnimeo, I., Corso, A.D., de Gironcoli, S., Delugas, P., DiStasio, R.A., Ferretti, A., Floris, A., Fratesi, G., Fugallo, G., Gebauer, R., Gerstmann, U., Giustino, F., Gorni, T., Jia, J., Kawamura, M., Ko, H.-Y., Kokalj, A., Küçükbenli, E., Lazzeri, M., Marsili, M., Marzari, N., Mauri, F., Nguyen, N.L., Nguyen, H.-V., de-la Roza, A.O., Paulatto, L., Poncé, S., Rocca, D., Sabatini, R., Santra, B., Schlipf, M., Seitsonen, A.P., Smogunov, A., Timrov, I., Thonhauser, T., Umari, P., Vast, N., Wu, X., Baroni, S., 2017. Advanced capabilities for materials modelling with quantum ESPRESSO. J. Phys.: Condens. Matter. 29 (46), 465901. http://dx.doi.org/10.1088/1361-648x/aa8f79.

Giannozzi, P., Baroni, S., Bonini, N., Calandra, M., Car, R., Cavazzoni, C., Ceresoli, D., Chiarotti, G.L., Cococcioni, M., Dabo, I., Dal Corso, A., de Gironcoli, S., Fabris, S., Fratesi, G., Gebauer, R., Gerstmann, U., Gougoussis, C., Kokalj, A., Lazzeri, M., Martin-Samos, L., Marzari, N., Mauri, F., Mazzarello, R., Paolini, S., Pasquarello, A., Paulatto, L., Sbraccia, C., Scandolo, S., Sclauzero, G., Seitsonen, A.P., Smogunov, A., Umari, P., Wentzcovitch, R.M., 2009. QUANTUM ESPRESSO: a modular and open-source software project for quantum simulations of materials. J. Phys.: Condens. Matter. 21 (39), 395502. http://dx.doi.org/10.1088/0953-8984/21/39/395502.

Granja-DelRío, A., Cabria, I., 2024a. Grand canonical Monte Carlo simulations of hydrogen and methane storage capacities of two novel Al-nia MOFs at room temperature. Int. J. Hydrog. Energy 50, 685–696. http://dx.doi.org/10.1016/j.ijhydene.2023.08.023.

Granja-DelRío, A., Cabria, I., 2024b. Insights into hydrogen and methane storage capacities: Grand canonical Monte Carlo simulations of SIGSUA. J. Chem. Phys. 2024, 154712. http://dx.doi.org/10.1063/5.0193291.

Grimme, S., Antony, J., Ehrlich, S., Krieg, H., 2010. A consistent and accurate ab initio parametrization of density functional dispersion correction (DFT-D) for the 94 elements H-Pu. J. Chem. Phys. 132, 154104. http://dx.doi.org/10.1063/1.3382344.

Haranczyk, M., 2024. Zeo++: an open source software for performing high-throughput geometry-based analysis of porous materials and their voids. http://www.zeoplusplus.org, (Accessed 15October 2024), Last version: 0.3, June 20, 2017.

Hwang, H.T., Varma, A., 2014. Hydrogen storage for fuel cell vehicles. Curr. Opin. Chem. Eng. 5, 42–48. http://dx.doi.org/10.1016/j.coche.2014.04.004.

Jaramillo, D.E., Jiang, H.Z.H., Evans, H.A., Chakraborty, R., Furukawa, H., Brown, C.M., Head-Gordon, M., Long, J.R., 2021. Ambient-temperature hydrogen storage via vanadium(II)-dihydrogen complexation in a metal-organic framework. J. Am. Chem. Soc. 143 (16), 6248–6256. http://dx.doi.org/10.1021/jacs.1c01883.

Jose, R., Bangar, G., Pal, S., Rajaraman, G., 2023. Role of molecular modelling in the development of metal-organic framework for gas adsorption applications.. J. Chem. Sci. 135, 19. http://dx.doi.org/10.1007/s12039-022-02130-5.

Kokalj, A., 2024. Xcrysden: a crystalline and molecular structure visualisation program. http://www.xcrysden.org, (Accessed 28 December 2024), Last version: 1.6.2, October 28, 2019.

Lennard-Jones, J.E., 1924. On the determination of molecular fields. Proc. Roy. Soc. (London) A 106, 463–477. http://dx.doi.org/10.1098/rspa.1924.0082.

Li, A., 2022. Metal-organic frameworks-based hydrogen storage strategies and applications. J. Phys.: Conf. Ser. 2403 (1), 012022. http://dx.doi.org/10.1088/1742-6596/2403/1/012022.

Li, A., Bueno, R., Wiggin, S., Ward, S.C., Wood, P.A., Fairen-Jimenez, D., 2021. The launch of a freely accessible MOF CIF collection from the CSD. Matter 4, 1090–1106. http://dx.doi.org/10.1016/j.matt.2021.03.006.

Löwdin, P.O., 1950. On the non-orthogonality problem connected with the use of atomic wave functions in the theory of molecules and crystals. J. Chem. Phys. 18, 365–375. http://dx.doi.org/10.1063/1.1747632.

Martin, R.L., Haranczyk, M., 2014. Structure models of crystalline porous polymers: Construction, characterization and design. Cryst. Growth Des. 14, 2431–2440. http://dx.doi.org/10.1021/cg500158c.

Martin, R.L., Smit, B., Haranczyk, M., 2012. Addressing challenges of identifying geometrically diverse sets of crystalline porous materials. J. Chem. Inf. Model. 52, 308–318. http://dx.doi.org/10.1021/ci200386x.

Nath, K., Ahmed, A., Siegel, D.J., Matzger, A.J., 2022. Computational identification and experimental demonstration of high-performance methane sorbents. Angew. Chem. Int. Ed. 61 (25), e202203575. http://dx.doi.org/10.1002/anie.202203575.

Office of Energy Efficiency & Renewable Energy, Fuel Cell Technologies Office, 2018. DOE technical targets for onboard hydrogen storage for light-duty vehicles. https://www.energy.gov/eere/fuelcells/doe-technical-targets-onboard-hydrogen-storage-light-duty-vehicles, (Accessed 28 December 2024).

Office of Energy Efficiency & Renewable Energy, Hydrogen and Fuel Cell Technologies Office, 2022. High-pressure hydrogen tank testing. https://www.energy.gov/eere/fuelcells/high-pressure-hydrogen-tank-testing, (Accessed 28 December 2024).

Ongari, D., Boyd, P.G., Barthel, S., Witman, M., Haranczyk, M., Smit, B., 2017. Accurate characterization of the pore volume in microporous crystalline materials. Langmuir 33 (51), 14529–14538. http://dx.doi.org/10.1021/acs.langmuir.7b01682.

Peng, Y., Krungleviciute, V., Eryazici, I., Hupp, J.T., Farha, O.K., Yildirim, T., 2013. Methane storage in metal-organic frameworks: Current records, surprise findings, and challenges. J. Am. Chem. Soc. 135 (32), 11887–11894. http://dx.doi.org/10.1021/ja4045289.

Pinheiro, M., Martin, R.L., Rycroft, C.H., Haranczyk, M., 2013a. High accuracy geometric analysis of crystalline porous materials. CrystEngComm 15, 7531–7538. http://dx.doi.org/10.1039/C3CE41057A.

Pinheiro, M., Martin, R.L., Rycroft, C.H., Jones, A., Iglesia, E., Haranczyk, M., 2013b. Characterization and comparison of pore landscapes in crystalline porous materials. J. Mol. Graph. Model. 44, 208–219. http://dx.doi.org/10.1016/j.jmgm.2013.05.007.

Rasul, M., Hazrat, M., Sattar, M., Jahirul, M., Shearer, M., 2022. The future of hydrogen: Challenges on production, storage and applications. Energy Convers. Manag. 272, 116326. http://dx.doi.org/10.1016/j.enconman.2022.116326.

Rodrigues, N.M., Politi, J.R., Martins, J.B., 2022. Are metal dopant and ligands efficient to optimize the adsorption rate of CH_4, h_2 and h_2s on IRMOFs? Insights from factorial design. Comput. Mater. Sci. 210, 111438. http://dx.doi.org/10.1016/j.commatsci.2022.111438.

Saha, D., Deng, S., 2010. Hydrogen adsorption on metal-organic framework MOF-177. Tsinghua Sci. Technol. 15 (4), 363–376. http://dx.doi.org/10.1016/S1007-0214(10)70075-4.

Sherburne, M., 2022. Natural gas could bridge gap from gasoline to electric vehicles, thanks to metal-organic frameworks. https://news.umich.edu/natural-gas-could-bridge-gap-from-gasoline-to-electric-vehicles-thanks-to-metal-organic-frameworks, (Accessed 28 December 2024).

Soave, G., 1972. Equilibrium constants from a modified Redlich-Kwong equation of state. Chem. Eng. Sci. 27, 1197–1203.

for Standardization, I.O., 2006. ISO 15403-1:2006(en) natural gas — Natural gas for use as a compressed fuel for vehicles — Part 1: Designation of the quality. https://www.iso.org/obp/ui/#iso:std:iso:15403:-1:ed-1:v1:en, (Accessed 28 December 2024).

Suresh, K., Aulakh, D., Purewal, J., Siegel, D.J., Veenstra, M., Matzger, A.J., 2021. Optimizing hydrogen storage in MOFs through engineering of crystal morphology and control of crystal size. J. Am. Chem. Soc. 143 (28), 10727–10734. http://dx.doi.org/10.1021/jacs.1c04926.

Turner, P.J., Grace Development Team, 2024. Grace: a WYSIWYG 2D plotting tool. http://plasma-gate.weizmann.ac.il/Grace, (Accessed 28 December 2024), Last version: 5.1.25, February 15, 2015.

Wang, L., Chen, X., Du, H., Yuan, Y., Qu, H., Zou, M., 2018. First-principles investigation on hydrogen storage performance of Li, Na and K decorated borophene. Appl. Surf. Sci. (ISSN: 0169-4332) 427, 1030–1037. http://dx.doi.org/10.1016/j.apsusc.2017.08.126.

Willems, T.F., Rycroft, C.H., Kazi, M., Meza, J.C., Haranczyk, M., 2012. Algorithms and tools for high-throughput geometry-based analysis of crystalline porous materials. Microporous Mesoporous Mater. 149 (1), 134–141. http://dx.doi.org/10.1016/j.micromeso.2011.08.020.

Yabing, H., Zhou, W., Guodong, Q., Chen, B., 2014. Methane storage in metal-organic frameworks. Chem. Soc. Rev. 45, 5657–5678.

Yuan, L., Chen, Y., Kang, L., Zhang, C., Wang, D., Wang, C., Zhang, M., Wu, X., 2017. First-principles investigation of hydrogen storage capacity of Y-decorated porous graphene. Appl. Surf. Sci. (ISSN: 0169-4332) 399, 463–468. http://dx.doi.org/10.1016/j.apsusc.2016.12.054.

Yuan, L., Kang, L., Chen, Y., Wang, D., Gong, J., Wang, C., Zhang, M., Wu, X., 2018. Hydrogen storage capacity on Ti-decorated porous graphene: First-principles investigation. Appl. Surf. Sci. (ISSN: 0169-4332) 434, 843–849. http://dx.doi.org/10.1016/j.apsusc.2017.10.231.

Zhang, L., Jia, C., Bai, F., Wang, W., An, S., Zhao, K., Li, Z., Li, J., Sun, H., 2024. A comprehensive review of the promising clean energy carrier: Hydrogen production, transportation, storage, and utilization (HPTSU) technologies. Fuel 355, 129455. http://dx.doi.org/10.1016/j.fuel.2023.129455.

Zhao, Y., Cui, Y., Xie, L., Geng, K., Wu, J., Meng, X., Hou, H., 2023a. CCDC 2203440: Experimental crystal structure determination. http://dx.doi.org/10.5517/ccdc.csd.cc2cyvqx.

Zhao, Y., Cui, Y., Xie, L., Geng, K., Wu, J., Meng, X., Hou, H., 2023b. Rational construction of metal organic framework hybrid assemblies for visible light-driven CO_2 conversion. Inorg. Chem. 62, 1240. http://dx.doi.org/10.1021/acs.inorgchem.2c03970.

Zhao, D., Wang, X., Yue, L., He, Y., Chen, B., 2022. Porous metal–organic frameworks for hydrogen storage. Chem. Commun. 58, 11059–11078. http://dx.doi.org/10.1039/D2CC04036K.

Zhou, W., Wu, H., Hartman, M.R., Yildirim, T., 2007. Hydrogen and methane adsorption in metal-organic frameworks: A high-pressure volumetric study. J. Phys. Chem. C 111 (44), 16131–16137. http://dx.doi.org/10.1021/jp074889i.